

Free-Volume Distributions of an Epoxy Polymer Probed by Positron Annihilation: Pressure Dependence

Q. Deng and Y. C. Jean*

Department of Chemistry, University of Missouri—Kansas City,
Kansas City, Missouri 64110

Received May 1, 1992; Revised Manuscript Received October 3, 1992

ABSTRACT: Positron annihilation spectroscopy has been applied to measure the free-volume hole distributions in an epoxy (DGEBA/DDH/DAB) polymer ($T_g = 62^\circ\text{C}$) as a function of quasi-isotropic pressure in the range of 0–14 kbar. The hole radius and volume distributions determined from orthopositronium lifetime distributions are found to be dramatically shifted to small values and to be narrower as a function of pressure. The hole radius distributions are found to be between 3.5 and 0.5 Å and to have maxima at 2.45, 2.02, 1.40, and 0.78 Å under the external pressure of 0.001, 1.8, 4.9, and 14.0 kbar, respectively.

Introduction

Studies of the microscopic free-volume properties at molecular and atomic scales can provide a basic understanding of the mechanical and physical properties of polymers. The theory of free volumes in polymers has been used to explain the thermal and mechanical behaviors of glass materials.¹ In recent years, a new microanalytical probe, positron annihilation spectroscopy (PAS), has been developed to probe the free-volume hole properties in polymeric materials.² In a series of experiments, we^{3–7} have determined the free-volume mean size, fraction, and anisotropic structure⁵ in polymers as a function of pressure, temperature, and time using the positron annihilation lifetime (PAL) method. The high sensitivity of PAS in probing free-volume properties arises from the fact that the positronium atom (Ps, a positron–electron bound state) is preferentially trapped (localized) in atomic-scale free-volume holes. Thus the observed positron annihilation signals directly originate from free-volume regions and are not interfered with by the bulk properties.

Recently,⁸ after further developing the PAL method by Laplace inversion of a PAL spectrum into a continuous lifetime distribution, we reported the free-volume distributions in an epoxy as a function of temperature. The results show that the hole radii are distributed in the range of 1–4 Å at room temperature in a Gaussian-type function and the distributions are shifted to a larger radius as the temperature increases.

Pressure can significantly change the physical structures of polymers. Increasing pressure causes a compression or a collapsing of free-volume holes. Large variations of Ps lifetime with pressure in liquids and polymeric systems were reported quite long ago.^{9,10} Recently,⁷ we reported the mean hole sizes as a function of pressure in an epoxy polymer (DGEBA/DDH/DAB). However, in reality, it is known that free volumes in polymers exist in a distribution function. In this work we have applied the recently developed PAL method to measure the orthopositronium distributions and reported the free-volume radius and volume distributions as a function of pressure up to 14.0 kbar.

Experimental Section

Epoxy Samples. The epoxy samples used in this study are the same as those reported in our temperature-dependence study.⁸ They are amine-cured epoxies consisting of the diglycidyl ether of Bisphenol A (DGEBA) *N,N'*-dimethyl-1,6-diaminohexane (DDH), and 1,4-diaminobutane (DAB) (Imperial Chemical Inc.) at an equivalent ratio of 5.0:2.8:2.2. A T_g of 62°C was determined

by a differential scanning calorimetry (DSC) measurement. Detailed descriptions of sample preparations can be found in our previous papers.^{3,8}

An anvil system and a hydraulic press (Carver Co.; up to 25-ton loads) were used to generate quasi-isotropic pressures up to 15 kbar. The principle of generating quasi-isotropic pressures follows the Bridgman method.¹¹ The outer diameter of the anvil was 25 mm with a working diameter of 14 mm, and the taper angle was 10° . Two epoxy samples (diameter 4 mm; thickness 1.0 mm) were housed in a gasket (19.0-mm o.d., made of pyrophyllite), which was precisely machined to match the sizes of the samples. A uniformly distributed isotropic pressure can be achieved for a working diameter/sample thickness ratio of 14:1.¹² In our experiment, the diameter/thickness ratio was 7:1 so that the pressure exerted on the samples is considered to be quasi-isotropic. Detailed descriptions of the pressure system can be found in our previous paper.⁷

Positron Annihilation Lifetime (PAL) Spectroscopy. A 25- μCi positron source ($^{22}\text{NaCl}$ from Du Pont) was directly deposited on one surface of the samples. All positron annihilation took place within a 1.0-mm radius of the source. The positron lifetime measurements were performed using a conventional fast-fast coincidence method.¹³ The time resolution of the lifetime apparatus was found to be 300 ps as monitored by using a ^{60}Co source. The lifetime spectra were collected at a counting rate of 180 cps, under static pressures of 0.001, 1.8, 4.9, and 14.0 kbar at 25°C . After the pressure was released, a lifetime spectrum was obtained to detect any hysteresis and relaxation effect on polymer molecular chains. Several spectra $((1-15) \times 10^6 \text{ counts})$ were collected at each pressure for a complete data analysis of lifetime distributions.

In PAL, the experimental measured positron annihilation rate λ is defined as an integration of the positron density $\rho_+(\mathbf{r})$ and the electron density $\rho_-(\mathbf{r})$:

$$\lambda = \text{const} \int \rho_-(\mathbf{r})\rho_+(\mathbf{r}) d\mathbf{r} \quad (1)$$

where const is a normalization constant related to the number of electrons involved in the annihilation process. The annihilation lifetime τ is the reciprocal of the annihilation rate λ . In the free-volume model proposed for positron annihilation,¹⁴ Ps is considered to be confined in a free space between molecules. In common polymers, where no Ps quenching functional groups exist in their molecular structures, it is expected that the orthopositronium (oPs, the triplet state) lifetime directly correlates with the hole size. By developing eq 1 based on a simple "particle in a spherical box", a correlation between the measured oPs annihilation lifetime τ_3 and hole radius R was obtained:^{15–17}

$$\tau_3 = \frac{1}{\lambda_3} = \frac{1}{2} \left[1 - \frac{R}{R_0} + \frac{1}{2\pi} \sin \left(\frac{2\pi R}{R_0} \right) \right]^{-1} \quad (2)$$

where τ_3 (oPs lifetime) and R (hole radius) are expressed in nanoseconds and angstroms, respectively. R_0 equals $R + \Delta R$, where ΔR is the electron layer thickness ($\Delta R = 1.66 \text{ Å}$).

Although the above equation is based on a crude quantum model, a more accurate theoretical model¹⁷ based on a finite potential shows that the above equation is still valid and most convenient for practical applications, as long as the empirical parameter, i.e., electron layer thickness = 1.66 Å, is well fitted between the known cavity radii and the measured oPs lifetimes. On the basis of eq 2, the radius of free-volume holes in polymers can be determined by measuring their oPs annihilation lifetime.

Data Analysis. All experimental PAL spectra have been analyzed by using two methods: a finite-term lifetime analysis and a continuous lifetime analysis.

(1) **Finite-Term Lifetime Analysis.** In conventional data analysis, an experimental PAL spectrum is expressed as a convoluted expression (symbol *) of the instrument resolution function and a finite number (n) of negative exponentials:

$$y(t) = R(t) * (N_t \sum_{i=1}^n \alpha_i \lambda_i e^{-\lambda_i t} + B) \quad (3)$$

where $y(t)$ is an experimental raw datum, $R(t)$ is the instrument resolution function, N_t is the normalized total count, B is the background, λ_i is the inverse of the i th lifetime component (τ_i), and $\alpha_i \lambda_i$ is its intensity. Practically, the number of resolvable terms (n) is limited to 2–5 because the resolution function is an unknown and cannot be measured exactly. An experimental spectrum $y(t)$ is then least-squares fitted to eq 3 to obtain lifetimes $\tau_i (=1/\lambda_i)$ and corresponding intensities $\alpha_i \lambda_i$. In epoxy samples, we found that $n = 3$ results give the best χ^2 (<1.1) and most reasonable standard deviations with commercially available computer codes POSITRONFIT and RESOLUTION in a PATFIT package.¹⁸

(2) **Continuous Lifetime Analysis.** Since free-volume holes exist in a form of distribution, oPs lifetimes should be expressed in a distribution instead of a discrete value. Hence, we express a positron lifetime spectrum in a continuous form originally suggested by Schrader¹⁹ as

$$Y(t) = R(t) * (N(t) \int_0^\infty \alpha(\lambda) \lambda e^{-\lambda t} d\lambda + B) \quad (4)$$

Finding the exact solution of $\alpha(\lambda) \cdot \lambda$, the probability density function (pdf) directly for the above equation, is a very difficult problem because the actual experimental spectra are convoluted by the unknown resolution function. However, if one measures a reference spectrum $Y_r(t)$, which has a known single positron decay rate (λ_r), the solution can be obtained by using $Y_r(t)$ to deconvolute positron spectra $Y(t)$. In this case, Y_r is expressed as

$$y_r(t) = R(t) * N_r \lambda_r e^{-\lambda_r t} \quad (5)$$

where N_r is the normalized total count for a reference spectrum and λ_r is the reciprocal of the known single lifetime (τ_r) from the reference sample. Only under the circumstance where the measurement of reference spectra is under the same experimental conditions as that of samples can the solutions of λ and $\lambda\alpha$ be resolved correctly. The deconvolution procedure performed by a Laplace inversion technique can be achieved by using a computer code named CONTIN, which was originally developed by Provencher²⁰ for fluorescence spectroscopic applications. Gregory and Zhu²¹ modified the code for use in positron annihilation spectroscopy. Advantages and precautions in using this CONTIN program for PAL have been described in our previous paper.⁸

Results and Discussion

PAL spectra of epoxy samples have been obtained at four different pressures with totals of 1×10^6 , 5×10^6 , 10×10^6 , and 15×10^6 counts. As shown in Figure 1, pressure has a big effect on the positron annihilation decay spectra, particularly on the long-lived components.

First, we use a conventional program, the PATFIT package,¹⁸ to fit the PAL spectra into three lifetimes according to eq 3. The lifetimes τ_i and corresponding intensities $I_i (= \alpha_i \lambda_i$ of eq 3) are listed in Table I. In order to obtain a consistent result for τ_2 and τ_3 , we have constrained $\tau_1 = 120$ ps in our final analysis. The χ^2 from

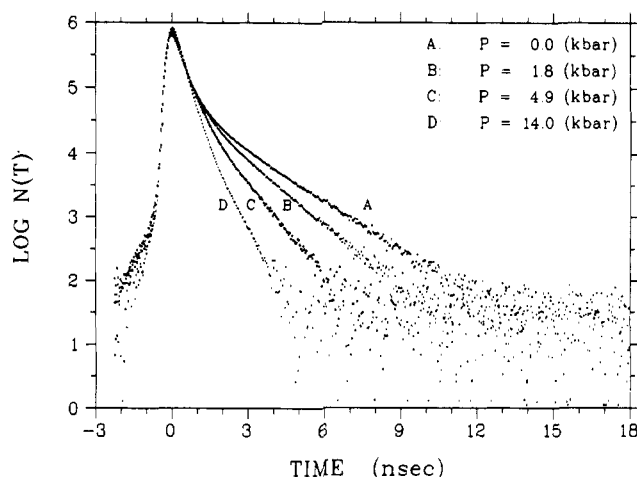


Figure 1. Raw positron lifetime spectra of an epoxy under quasi-isotropic pressures at 25 °C. The total counts for each spectrum are 15×10^6 .

the unconstrained and the constrained results are essentially the same but τ_2 , I_1 , and I_2 are consistent and stable for the constrained rather than for the unconstrained results. Three lifetimes correspond to three states of positron and Ps existence in epoxies: the shortest lifetime, $\tau_1 = 0.120$ ns, is attributed to pPs (singlet Ps) annihilation; the second lifetime, $\tau_2 = 0.26$ – 0.35 ns, is mainly due to positron (not Ps) annihilation; and the long lifetime, $\tau_3 = 0.6$ – 1.6 ns, is due to oPs (triplet Ps) annihilation. Mean values of free volumes are then calculated by using τ_3 and eq 2, and the results are listed in Table I. We note that both τ_2 and τ_3 decrease in a similar way as the pressure increases, indicating that Ps and the positron behave similarly in polymers, both localized in free-volume holes.

In order to obtain free-volume distributions, we employ the CONTIN program^{20,21} to fit the PAL spectra into continuous lifetimes based on eqs 4 and 5. In this method, we use four reference samples: a well-annealed single crystal Al ($\tau = 162$ ps, 98%), an ultrahigh-purity polycrystalline Ni ($\tau = 110$ ps, 98%), a single crystal Cu ($\tau = 121$ ps, 99%), and a ²⁰⁷Bi radioisotope (10 μ Ci from Radioisotope Corp.; it emits two γ -rays with energies very close to ²²Na) to deconvolute the lifetime spectra. All these reference spectra give consistent results for lifetime distributions. In Figure 2, the positron annihilation lifetime probability density functions, $\alpha(\lambda) \cdot \lambda^2$, of epoxy samples are plotted vs lifetime, τ , under four different pressures. Each spectrum contains a total of 15×10^6 counts, and the reference spectrum was a lifetime spectrum of single crystal Al. The lifetime distributions have been normalized to 1 over the entire probability density functions output from the CONTIN program.

As shown in Figure 2, the results from three peaks resolved by CONTIN algorithm agree with three discrete lifetimes resolved by PATFIT algorithm. In general, the lifetime results agree with those obtained by PATFIT analysis as listed in Table I. However, there exists some detailed differences between them, particularly the results for short-lifetime components. In order to make a quantitative comparison, we calculate the mean positron lifetimes and intensities for the CONTIN results ($\bar{\tau}_i$ and \bar{I}_i , $i = 1$ – 3) by integrating the data of Figure 2 between the lifetime intervals τ_a and τ_b for each peak defined as

$$\bar{\tau}_i = \int_{\tau_a}^{\tau_b} \alpha_i \lambda_i^2 \tau_i d\tau_i / \int_{\tau_a}^{\tau_b} \alpha_i \lambda_i^2 d\tau_i$$

$$\bar{I}_i = \int_{\tau_a}^{\tau_b} \alpha_i \lambda_i^2 d\tau_i \quad (6)$$

Table I
Positron and Positronium Lifetime Results Obtained by Finite-Term Analysis in an Epoxy Polymer

| pressure (kbar) | τ_1 (ps) | τ_2 (ps) | τ_3 (ps) | I_1 (%) | I_2 (%) | I_3 (%) | R^c (Å) |
|------------------|---------------|---------------|---------------|------------|------------|------------|------------|
| 0.0 ^a | 120 | 367 | 1632 | 16.15 | 59.38 | 24.47 | 2.49 |
| | ± 0 | ± 3 | ± 11 | ± 0.55 | ± 0.46 | ± 0.23 | ± 0.01 |
| 1.8 | 120 | 342 | 1255 | 14.23 | 61.36 | 24.41 | 2.03 |
| ± 0.1 | ± 0 | ± 3 | ± 8 | ± 0.55 | ± 0.43 | ± 0.28 | ± 0.01 |
| 4.9 | 120 | 307 | 871 | 14.24 | 65.31 | 20.45 | 1.43 |
| ± 0.1 | ± 0 | ± 4 | ± 11 | ± 0.85 | ± 0.62 | ± 0.60 | ± 0.02 |
| 14.0 | 120 | 267 | 588 | 11.92 | 72.07 | 16.01 | 0.72 |
| ± 0.1 | ± 0 | ± 7 | ± 20 | ± 1.75 | ± 1.23 | ± 1.85 | ± 0.05 |
| 0.0 ^b | 120 | 369 | 1635 | 16.13 | 59.43 | 24.45 | 2.49 |
| | ± 0 | ± 3 | ± 9 | ± 0.45 | ± 0.37 | ± 0.20 | ± 0.01 |

^a Before applying pressure. ^b After applying pressure (10 days after releasing pressure). ^c R are the mean free-volume hole radii obtained by using τ_3 according to eq 2.

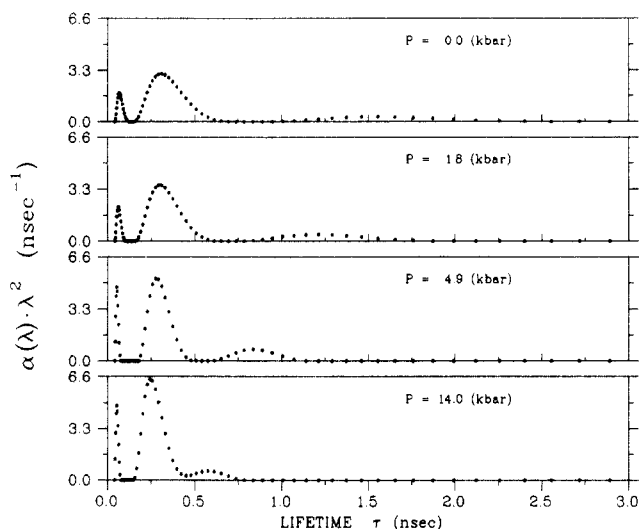


Figure 2. Lifetime distributions of an epoxy polymer at 25 °C under quasi-isotropic pressure. The distributions were obtained by using the Laplace inversion program CONTIN.

The results of $\bar{\tau}_1$, $\bar{\tau}_2$, $\bar{\tau}_3$, \bar{I}_1 , \bar{I}_2 , and \bar{I}_3 at different pressures are listed in Table II. Comparing the results listed in Tables I and II, we make the following observations: (1) $\bar{\tau}_3$ and τ_3 are the same, (2) $\bar{\tau}_2$ is slightly lower than τ_2 , (3) $\bar{\tau}_1$ is significantly less than τ_1 , (4) \bar{I}_3 and I_3 are the same, and (5) \bar{I}_1 is significantly less than I_1 , but closer to $1/3$ of \bar{I}_3 . Similar discrepancies in the short-lifetime results are also found in our temperature-dependence results.⁸ These discrepancies result from the limited instrument resolution (≈ 0.25 – 0.35 ns). In the PATFIT algorithm, τ_1 , τ_2 , I_1 , and I_2 are known to be highly correlated; i.e., correlation coefficients are in the range of 0.7–0.9. It is not surprising that the results from two independent algorithms show such discrepancies in the short-lived results. On the other hand, when we take the mean values of τ_1 and τ_2 defined as $\bar{\tau}_{1,2} = \tau_1 I_1 + \tau_2 I_2$, we find the $\bar{\tau}_{1,2}$ results obtained from CONTIN are essentially the same as the results from PATFIT (within 8 ps). This comparison indicates that one will have to take precautions in interpreting the short-lifetime results obtained by using PATFIT analysis on a spectrum which contains multilifetime components. Here we employ the longest lifetime results (oPs lifetime distributions), which are not affected by the instrument resolution, to interpret free-volume distributions. For the purpose of clarity, the oPs distributions from Figure 2 are replotted in Figure 3. The oPs lifetime distributions $\alpha(\lambda) \cdot \lambda^2$ are found to be narrower as the pressure increases.

Another interesting result is the distribution of positron lifetimes (the center peaks of Figure 2). Recently, we found that both the Ps atom and positrons are localized at free-volume holes in polymers.⁷ Thus we expect that the

positron lifetimes will also have a distribution similar to oPs and will vary as a function of pressure. As shown in Figure 4, which is a replot of the middle peaks from Figure 2, the distributions of the positron lifetimes shift in a way similar to oPs lifetime (Figure 3) shifts. This gives further evidence that the positron is also localized in free-volume holes. The localization of the positron in polymers may bring practical applications of PAS to certain polymeric materials where no oPs is formed, such as conducting polymers. In the current work, the results of the oPs lifetime distribution are employed to interpret the free-volume hole distribution with a higher accuracy than using the positron lifetime distribution. Before we convert the distribution density function $\alpha(\lambda) \cdot \lambda^2$ to the radius distribution function using eq 2, we need to consider some possible effects due to a Ps probe in a free-volume hole. First, what is the possibility of Ps probing more than one hole before it annihilates? We argue that this is unlikely from the view of the large Ps-binding energies with holes (in the order of 0.5 eV).¹³ The chance of the Ps escaping from a hole or diffusing to another before it annihilates is almost zero. Second, what is the possibility that the Ps creates additional spaces when it is localized in a preexisting free-volume hole? Although it is known that the Ps creates bubbles in liquids, we argue that the Ps does not create additional spaces in glassy polymers because its rigid structure is much like of a solid state. This is supported by the fact²² that no Ps bubble has been observed in any solid with the exception of solid He. Third, what is the effect of the Ps trapping probability as a function of hole size? A larger hole is expected to have a larger Ps trapping (or capture) probability than a small hole. The exact relationship between the Ps capture probability and the hole size has not been reported. However, the relationship between the trapping rate of the positron and the hole size in voids has been reported.²³ It is nearly a linear function for a radius up to about 6 Å. Since Ps and the positron behave similarly in their trapping properties to the free volumes of polymers, we have developed a correction factor $K(R)$ for the Ps trapping probability as a function of hole radius R from the positron trapping-void size relationship as²⁴

$$K(R) = 1.0 + 8.0R \quad (7)$$

where 8.0 is taken from the ratio between the positron trapping rate and the hole radius of voids²³ and R is expressed in angstroms. After considering the difference of oPs capture probability in different hole sizes, we obtain an expression for the free-volume hole radius probability density function, $f(R)$, defined as $[-\alpha(\lambda) d\lambda_3/dR]/K(R)$ to

Table II
Mean Values of Positron and Positronium Lifetime Integrated from the Continuous Lifetime Results in an Epoxy Polymer

| pressure (kbar) | $\bar{\tau}_1$ (ps) | $\bar{\tau}_2$ (ps) | $\bar{\tau}_3$ (ps) | I_1 (%) | I_2 (%) | I_3 (%) | \bar{R}^c (Å) |
|------------------|---------------------|---------------------|---------------------|-----------|-----------|-----------|-----------------|
| 0.0 ^a | 100 | 351 | 1630 | 6.36 | 68.68 | 24.96 | 2.48 |
| 1.8 | 76 | 330 | 1251 | 5.90 | 70.25 | 23.85 | 2.03 |
| 4.9 | 67 | 295 | 862 | 7.63 | 71.44 | 20.93 | 1.41 |
| 14.0 | 58 | 259 | 592 | 7.41 | 77.49 | 15.10 | 0.73 |
| 0.0 ^b | 80 | 351 | 1621 | 7.19 | 68.35 | 24.46 | 2.47 |

^a Before applying pressure. ^b After applying pressure (10 days after releasing pressure). ^c \bar{R} are the mean free-volume hole radii obtained by using τ_3 according to eq 2.

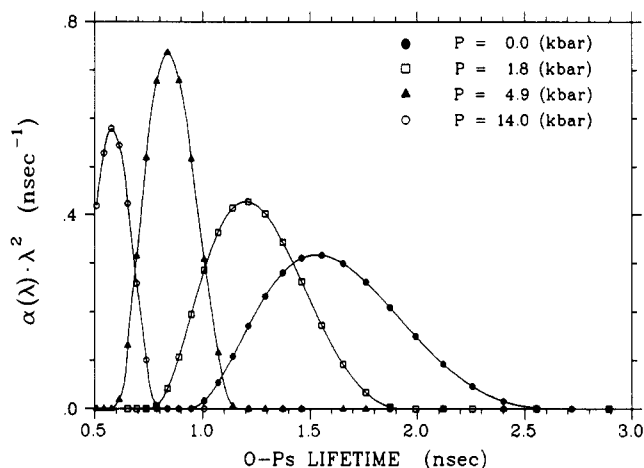


Figure 3. oPs lifetime distributions of an epoxy polymer. The data are from the right-hand peaks shown in Figure 2.

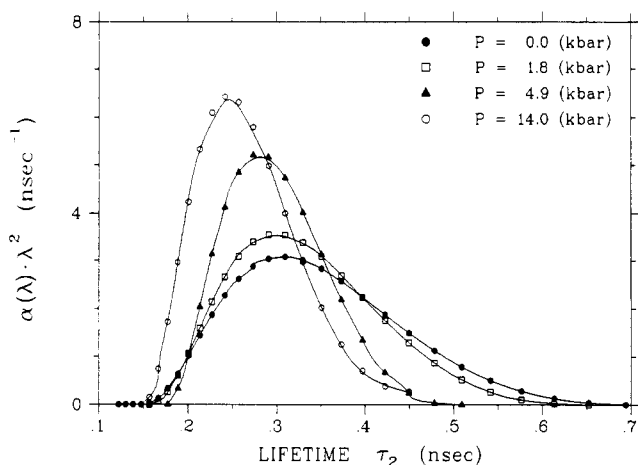


Figure 4. Positron lifetime distributions of an epoxy polymer. The data are from the middle peaks shown in Figure 2.

be²⁴

$$f(R) = -3.32 \{ \cos [2\pi R / (R + 1.66)] - 1 \} \alpha(\lambda) / [(R + 1.66)^2] K(R) \quad (8)$$

The fraction of oPs annihilating in the holes with radii between R and dR is $f(R) dR$. The results of the radius probability distribution function, $f(R)$, calculated according to eq (8) for the data shown in Figure 3 at 0.001, 1.8, 4.9, and 14.0 kbar, are plotted in Figure 5. As shown in Figure 5, the hole radius distribution functions are found to be fairly symmetric and narrow. They can be approximately expressed by a single gaussian function with full width at half-maximum (fwhm) of ca. 0.6–0.9 Å. As expected, an increase in pressure results in a collapsing and a compressing of the free-volume holes, the peak maxima of hole distributions shift from 2.45 Å to 2.0, 1.4, and 0.8 Å for 1.8, 4.9, and 14.0 kbar, respectively, and the peak shapes become narrower. We note a distorted distribution for very small hole regions is shown in Figure 5 for $P = 14.0$ kbar. This is because the hole radius has

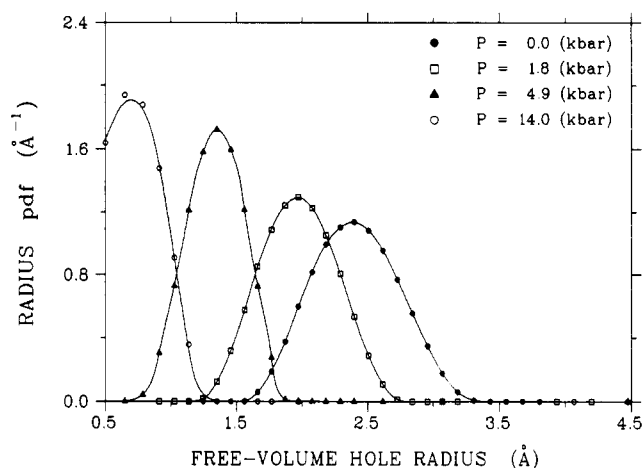


Figure 5. Free-volume hole radius distribution functions $f(R)$ of an epoxy polymer under different pressures. Smooth curves are drawn through data points merely for clarity.

been squeezed to the limiting value of ca. 0.5 Å, which the Ps can probe properly. The limiting hole size of the Ps probe (ca. 2×0.5 Å) results from (1) the Bohr diameter of Ps, 1.06 Å, (2) convergence of the oPs lifetime (near 0.5 ns) with that of the positron lifetime, and (3) a decrease of capture rate/probability of Ps as the hole size becomes very small. Our results of radius distributions of free-volume hole are about in the same order of magnitude as the interatomic distances in hydrocarbons and are consistent with the results obtained from molecular dynamic simulation²⁵ (2–3 Å radius).

It is also of interest to report the hole volume probability density function (pdf) for theoretical comparisons in the future. The hole volume pdf $g(V)$ can be obtained by assuming spherical holes and is expressed as

$$g(V) = f(R) / 4\pi R^2 \quad (9)$$

The fraction of hole volume distribution as determined by oPs annihilation in holes with volume between V and $V + dV$ is given by $g(V) dV$. The results for $g(V)$, from the $f(R)$ results of Figure 5 and eq 9, are plotted in Figure 6 for 0.001, 1.8, 4.9, and 14.0 kbar, respectively. The distributions of hole volumes are found to be skewed to the larger holes. As the pressure increases, distributions shift to smaller hole volumes and become narrower. The hole volume distributions shift from 16–160 Å³ at 0.001 kbar to 0–9 Å³ at 14.0 kbar.

The long tail distributions for the larger volumes (Figure 6) are found to be similar to an exponential function as theoretically simulated results by molecular dynamic methods in simple hydrocarbons²⁵ while the symmetric hole radius distribution functions (Figure 5) are found to be similar to γ -functions as theoretically calculated by kinetic theory.²⁶

Conclusions

We have reported the direct measurements of free-volume hole distributions in an epoxy polymer under four

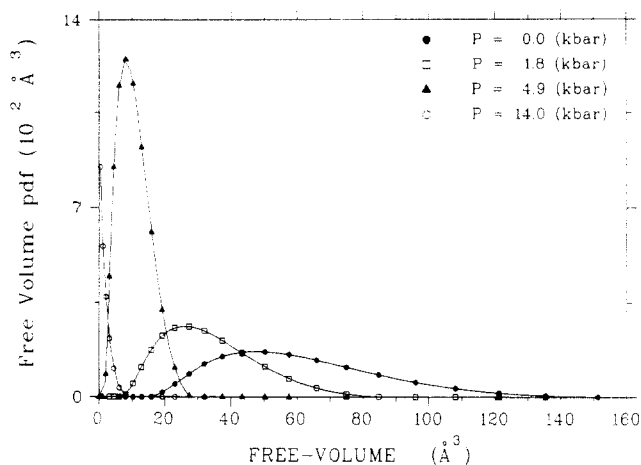


Figure 6. Hole volume distribution functions $g(V)$ of an epoxy polymer under different pressures. Smooth curves are drawn through data points merely for clarity.

different pressures at 25 °C. The hole volume distributions shift dramatically from a maximum 50 Å³ to 25, 8, and 1 Å³ for 1.8, 4.9, and 14.0 kbar, respectively. The width of the distribution is found to be narrowed as pressure increases. With successful Laplace inversion of the positron lifetime spectra into a continuous distribution as presented here, we expect that more quantitative information for polymeric material properties by using the PAL method will be forthcoming in the future.

Acknowledgment. This work has been supported by a grant from the National Science Foundation (DMR-9004083). Fruitful discussions with Prof. R. B. Gregory and Dr. T. C. Sandreczki are acknowledged.

References and Notes

- (1) Cohen, M. H.; Turnbull, D. *J. Chem. Phys.* **1959**, *31*, 1164.
- (2) For examples, see: Jean, Y. C. *Microchem. J.* **1990**, *42*, 72. Stevens, J. R. Probe and Label Techniques. In *Methods of Experimental Physics*; Fava, R. A., Ed.; Academic: London 1980; p 371.
- (3) Jean, Y. C.; Sandreczki, T. C.; Ames, D. P. *J. Polym. Sci. B* **1986**, *24*, 1247.
- (4) Nakanishi, H.; Jean, Y. C.; Smith, E. G.; Sandreczki, T. C. *J. Polym. Sci. B* **1989**, *27*, 1419.
- (5) Jean, Y. C.; Nakanishi, H.; Hao, L. Y.; Sandreczki, T. C. *Phys. Rev. B* **1990**, *42*, 9705.
- (6) Wang, Y. Y.; Nakanishi, H.; Jean, Y. C.; Sandreczki, T. C. *J. Polym. Sci. B* **1990**, *28*, 1431.
- (7) Deng, Q.; Sundar, C. S.; Jean, Y. C. *J. Phys. Chem.* **1992**, *96*, 492.
- (8) Deng, Q.; Zandiehndem, F.; Jean, Y. C. *Macromolecules* **1992**, *25*, 1090.
- (9) Wilson, R. K.; Johnson, P. O.; Stump, R. *Phys. Rev.* **1963**, *129*, 2091.
- (10) Hautajarvi, P.; Rytola, K.; Tnovinoi, P.; Jauko, P. *Phys. Lett.* **1976**, *57A*, 175.
- (11) Bridgman, P. W. *The Physics of High Pressure*; G. Bell and Sons, Ltd.: London, 1949.
- (12) Dacheille, F.; Roy, R. *Modern Very High Pressure Technique*; Wentorf, R. H., Ed.; Butterworths: Washington, DC, 1962; p 163.
- (13) For example, see: *Positron Solid-State Physics*; Brandt, W., Dupasquier, A., Eds.; North Holland: Amsterdam, 1983. *Positron and Positronium Chemistry*; Schrader, D. M., Jean, Y. C., Eds.; Elsevier: Amsterdam, 1988.
- (14) Brandt, W.; Berko, S.; Walker, W. W. *Phys. Rev.* **1960**, *12*, 1289.
- (15) Tao, S. J. *J. Chem. Phys.* **1972**, *56*, 5499.
- (16) Eldrup, M.; Lightbody, D.; Sherwood, J. N. *Chem. Phys.* **1981**, *63*, 51.
- (17) Nakanishi, H.; Wang, S. J.; Jean, Y. C. In *Positron Annihilation Studies of Fluids*; Sharma, S. C., Ed.; World Science: Singapore, 1988; p 292.
- (18) PATFIT package Risø National Laboratory, Roskilde, Denmark, 1989.
- (19) Schrader, D. M. In *Positron Annihilation*; Coleman, P. G., Sharma, S. C., Diana, L. M., Eds.; North-Holland: Amsterdam, 1982; pp 912-914.
- (20) Provencher, S. W. CONTIN program, EMBL Technical Report DA05, European Molecular Biology Laboratory, Heidelberg, Germany, 1982; *Comput. Phys. Commun.* **1982**, *27*, 229.
- (21) Gregory, R. B.; Zhu, Y. *Nucl. Instrum. Methods Phys. Res.* **1990**, *A290*, 172.
- (22) Stewart, A. T.; Briscoe, C. V.; Steinbacher, J. J. *Can. J. Phys.* **1990**, *68*, 1362.
- (23) Nieminen, R. M. In *Positron Solid-State Physics*; Brandt, W., Dupasquier, A., Eds.; North Holland: Amsterdam, 1983; p 385.
- (24) Jean, Y. C.; Deng, Q. *J. Polym. Sci. B*, **1992**, *29*, 1359.
- (25) Rigby, D.; Roe, R. J. *Macromolecules* **1990**, *23*, 5312.
- (26) Robertson, R. E.; Simha, R.; Curro, J. G. *Macromolecules* **1988**, *18*, 2239.